Local Structure at the Air/Liquid Interface of Room-Temperature Ionic Liquids Probed by Infrared–Visible Sum Frequency Generation Vibrational Spectroscopy: 1-Alkyl-3-methylimidazol...

ARTICLE *in* THE JOURNAL OF PHYSICAL CHEMISTRY B · MAY 2007

Impact Factor: 3.3 · DOI: 10.1021/jp067162n · Source: PubMed

Local Structure at the Air/Liquid Interface of Room-Temperature Ionic Liquids Probed by Infrared−Visible Sum Frequency Generation Vibrational Spectroscopy: 1-Alkyl-3-methylimidazolium Tetrafluoroborates†

Toshifumi Iimori,[‡,#] Takashi Iwahashi,[§] Kaname Kanai,[§] Kazuhiko Seki,[§] Jaeho Sung,[⊥] Doseok Kim,[⊥] Hiro-o Hamaguchi,[||] and Yukio Ouchi*[,§]

Research Center for Materials Science, Nagoya University, Furo-cho, Chikusa-ku, Nagoya 464-8602, Japan, Department of Chemistry, Graduate School of Science, Nagoya University, Furo-cho, Chikusa-ku, Nagoya 464-8602, Japan, Department of Physics and Interdisciplinary Program of Integrated Biotechnology, Sogang University, Sinsoo-Dong, Mapo-Gu, Seoul 121-742, Republic of Korea, Department of Chemistry, School of Science, The University of Tokyo, 7-3-1, Hongo, Bunkyo-ku, Tokyo 113-0033, Japan

Received: October 31, 2006; In Final Form: March 3, 2007

The air/liquid interface of 1-alkyl-3-methylimidazolium tetrafluoroborates with the general formula $[C_n\text{mim}]BF_4$ ($n = 4-11$) was studied using infrared−visible sum frequency generation (SFG) vibrational spectroscopy. The probability of the gauche defect per CH_2-CH_2 bond in the alkyl chain decreases as the number of carbon atoms in the alkyl chain increases. This observation suggests that the interaction between the alkyl chains is enhanced as the alkyl chain length becomes longer. The frequencies of the C−H stretching vibrational modes observed in the SFG spectra are higher than those of the corresponding peak positions observed in the infrared spectra of the bulk liquids. This shift is consistent with a structure in which the alkyl chain protrudes from the bulk liquid into the air. A local structure, which originates from the intermolecular interaction between the ionic liquid molecules, is proposed to explain these observations.

1. Introduction

Room-temperature ionic liquids are salts that have melting points lower than room temperature at ambient pressure. Many ionic liquids are durable against moisture and air and have been actively studied as advantageous solvents for chemical syntheses, including organometallic catalysis reactions, enzyme catalysis reactions, and electrooxidation.[1−8] They can be also utilized as new fluids for numerous industrial products, including lithium ion batteries,[9,10] capacitors,[11,12] and fuel cell electrolytes.[13,14] The functionality of ionic liquids stems from the fact that ionic liquids are good solvents for many chemicals and are solvents that show negligible vapor pressures and have high ion transportation and a wide electrochemical window. In particular, room-temperature ionic liquids, which consist of the 1-alkyl-3-methylimidazolium cations (denoted by $[C_n\text{mim}]^+$, where C_n represents the alkyl chain with the formula $C_nH_{2n+1}-$) and various anions, have been intensively studied.[15−19] Although the number of reports related to room-temperature ionic liquid applications has rapidly and markedly increased, attempts to understand the fundamental aspects of ionic liquids remain limited.

Clarification of the molecular structure and the microscopic state, or structural characterization, is extremely important to understand the physical and chemical properties of materials. Crystal structure analysis of $[C_4\text{mim}]Cl$ has shown that hydrogen-bonding and Coulombic electrostatic interactions occur between the cation and the chloride anion, but the butyl chains are closely associated to create a hydrophobic region.[20,21] Raman vibrational spectroscopy, neutron diffraction measurements, and an X-ray scattering method have also been used to study the local structure in bulk ionic liquids.[22−25] These studies have demonstrated that the local structure resembles the packing structure found in a crystalline state. For ionic liquids based on the $[C_n\text{mim}]^+$ cation with different alkyl chain lengths, molecular dynamics simulations have been used to investigate the liquid structure.[26,27] These simulation studies indicated that the alkyl chain aggregates, whereas the charged anions and head groups of the cations are distributed homogeneously.

The effect of systematic modification of molecular structures on material properties has often been investigated because one can understand the interplay between the molecular structure and physical properties from such investigations. The effects of changing the alkyl chain length in $[C_n\text{mim}][(CF_3SO_2)_2N]$ as well as changing the anion species (X^-) in $[C_4\text{mim}]X$ on the physical properties of the liquids have been extensively studied by Watanabe et al.[15,16] By comparing properties such as molar conductivity between the ionic liquids with the various alkyl chain lengths, they have discussed the balance between the Coulombic attraction and an inductive force among the constituent molecules.

The interface structures of ionic liquids are also of emergent interest and have been investigated using various techniques, such as direct recoil spectrometry,[28] surface tension measurement,[29] neutron reflectometry and X-ray reflectivity measurement,[30,31] nonlinear surface spectroscopy,[32−35] and electron spectroscopy.[36] The interface properties of ionic liquids are important in applications such as electrochemistry,[37] phase-separable catalysis,[38,39] and extraction processes of chemicals.[5]

† Part of the special issue "Physical Chemistry of Ionic Liquids".

* Corresponding author. E-mail: ohuchi@mat.chem.nagoya-u.ac.jp.
‡ Research Center for Materials Science, Nagoya University.
§ Graduate School of Science, Nagoya University.
⊥ Sogang University.
|| The University of Tokyo.
Present address: Research Institute for Electronic Science, Hokkaido University, Sapporo 060-0812, Japan.

10.1021/jp067162n CCC: $37.00
Published on Web 04/12/2007

The comprehensive study on the interfacial structure in a series of room-temperature ionic liquids having different molecular structures should be valuable for understanding of the interface properties. However, such a study is still needed. Herein, we report the infrared (IR)-visible sum frequency generation (SFG) spectroscopy of the air/liquid interface of the room-temperature ionic liquids [$C_n$mim]BF_4 with different alkyl chains from $n =$ 4 to 11. The chain length dependence of the conformation disorder of the alkyl chain is derived from the SFG signal strength. In addition, the local ordering at the interface and its relation to the intermolecular interaction characteristic to the ionic liquid molecules are discussed.

2. Theoretical Background

The interaction of two optical waves in nonlinear media can generate a second-order nonlinear polarization. This nonlinear polarization is the source of the SFG process. SFG spectroscopy is a powerful tool to probe molecules at interfaces because the second-order nonlinear susceptibility is zero in isotropic media and, hence, surface- or interface-specific.[40,41] The basic theory of surface SFG spectroscopy has been described previously.[42] In usual surface SFG experiments, a visible beam at frequency ω_1 and a tunable IR beam at ω_2 are overlapped at the surface and generate the sum-frequency at the frequency $\omega_1 + \omega_2$. The observed SFG signal intensity [denoted by $I(\omega_1 + \omega_2)$] is proportional to the square modulus of an effective surface nonlinear susceptibility, $\chi^{(2)}_{\mathrm{eff}}$:

$$I(\omega_1 + \omega_2) \propto |\chi^{(2)}_{\mathrm{eff}}|^2 \tag{1}$$

In the above equation, $\chi^{(2)}_{\mathrm{eff}}$ is given by

$$\chi^{(2)}_{\mathrm{eff}} = [\hat{\mathbf{e}}(\omega_1 + \omega_2)L(\omega_1 + \omega_2)]\chi^{(2)}:[L(\omega_1)\cdot\hat{\mathbf{e}}(\omega_1)][L(\omega_2)\cdot\hat{\mathbf{e}}(\omega_2)] \tag{2}$$

where $\hat{\mathbf{e}}(\omega_1)$, $\hat{\mathbf{e}}(\omega_2)$, and $\hat{\mathbf{e}}(\omega_1 + \omega_2)$ are the unit polarization vectors for the input and output beams, respectively. $L(\omega_1)$, $L(\omega_2)$, and $L(\omega_1 + \omega_2)$ represent the Fresnel factors for the input and output beams, respectively. The Fresnel factor depends on both the geometry of the light beams and the refractive indices of the media. The calculation of the Fresnel factors for the ionic liquid [C_4mim]BF_4 has been already described elsewhere.[35] $\chi^{(2)}$ is the second-order nonlinear susceptibility of the surface and can be related to the hyperpolarizability, $\beta^{(2)}$, of the molecule in the form of

$$\chi^{(2)} = N_S\langle\beta^{(2)}\rangle \tag{3}$$

where N_S is the number density of molecules at the surface, and the angular brackets denote the average over the molecular orientational distribution. Under a resonant condition for ω_2, the ω_2 dependence of $\beta^{(2)}$ can be written as

$$\beta^{(2)} = \beta^{(2)}_{\mathrm{NR}} + \sum_q \frac{\alpha_q}{\omega_q - \omega_2 - i\Gamma_q} \tag{4}$$

where $\beta^{(2)}_{\mathrm{NR}}$ is the nonresonant contribution to $\beta^{(2)}$, q represents a vibrational mode, and α_q, ω_q, and Γ_q are the strength, the resonant frequency, and the damping constant of the vibrational mode, respectively. From the above relations, we have

$$\chi^{(2)}(\omega_2) = \chi^{(2)}_{\mathrm{NR}} + \sum_q \frac{A_q}{\omega_q - \omega_2 - i\Gamma_q} \tag{5}$$

where $\chi^{(2)}_{\mathrm{NR}}$ refers to a nonresonant component, and A_q is the strength.

By fitting eq 1 to the observed SFG spectra, the parameters of $A_{q,\mathrm{eff}}$, ω_q, and Γ_q can be experimentally obtained, where $A_{q,\mathrm{eff}}$ corresponds to the strength A_q multiplied by the appropriate Fresnel factors following eq 2.

In the case in which the surface or interface is two-dimensionally isotropic, the nonvanishing elements of $\chi^{(2)}$ are $\chi^{(2)}_{XXZ} = \chi^{(2)}_{YYZ}$, $\chi^{(2)}_{XZX} = \chi^{(2)}_{YZY}$, $\chi^{(2)}_{ZXX} = \chi^{(2)}_{ZYY}$, and $\chi^{(2)}_{ZZZ}$ where (X, Y, Z) is the laboratory coordinate system such that Z defines the interface normal, and the XZ plane is the incident plane. We measured the SFG signal using four different input and output polarization combinations: the ssp (denoting the s-polarized sum-frequency, s-polarized visible, and p-polarized IR fields, respectively), sps, pss, and ppp. The $\chi^{(2)}_{\mathrm{eff}}$'s probed using these polarization combinations can be expressed by linear combinations of the nonvanishing elements of $\chi^{(2)}$.[42]

3. Experimental Section

3.1. Preparation of Materials. Ionic liquids with various alkyl chain lengths were synthesized by slightly modifying previously reported methods.[18,43] [$C_n$mim]Br were prepared by the alkylation of 1-methylimidazole (Aldrich, purity 99+%, used as received) with an equimolar amount of $C_nH_{2n+1}Br$ (TCI, purity >98%, $n = 4-11$), which was distilled under low pressure. To prepare the ionic liquids for which $n = 4-9$, the reaction mixture was stirred at room temperature for 2−3 days. [$C_n$mim]Br, which were obtained as viscous liquids, were washed several times with ethyl acetate. An aqueous solution of [$C_n$mim]Br and a slight molar excess of $NaBF_4$ (Wako Chemical, purity 98%, used as received) was stirred at room temperature for 3 days. The produced [$C_n$mim]BF_4 were extracted from water using dichloromethane. After the extraction, dichloromethane was evaporated in vacuo. To prepare the ionic liquids having an alkyl chain length of $n = 10$ and 11, the reaction mixture of 1-methylimidazole and $C_nH_{2n+1}Br$ was stirred for 3−4 days. The produced [$C_n$mim]Br were washed with toluene. The ionic liquids [$C_n$mim]BF_4 were prepared by the above-mentioned anion substitution in water.

The colorless liquids [$C_n$mim]BF_4 were further degassed by repeatedly heating and cooling in vacuo for at least several hours to remove water and volatile solvent. The purity was verified using ^{1}H NMR spectroscopy. In the ^{1}H NMR spectra of the degassed products, water was an impurity (less than 9 mol % for [C_4mim]BF_4) due to the hygroscopic nature of the ionic liquids. The reactants, [$C_n$mim]Br, and the organic solvents did not appear in the ^{1}H NMR spectra.

3.2. Optical Setup and Measurements. A mode-locked, picosecond Nd:YAG laser (Ekspla, PL-2143B, 25 ps pulsewidth, 10 Hz) with a difference frequency generation (DFG) unit (Ekspla, DFG 401, mounting LBO and $AgGaS_2$ crystals) was used. The second harmonic of the Nd:YAG laser output was used as the input visible beam. A tunable IR laser pulse was generated using the DFG unit pumped by the third harmonic and fundamental of the Nd:YAG laser output. Typical input intensities were ~200 μJ/pulse for both the visible and IR beams, and the incident angles were 69° and 50°, respectively. The two beams were focused and overlapped at the surface of the ionic liquids in a glass vessel, and the outgoing SFG beam was filtered, depolarized, detected by a photomultiplier tube,

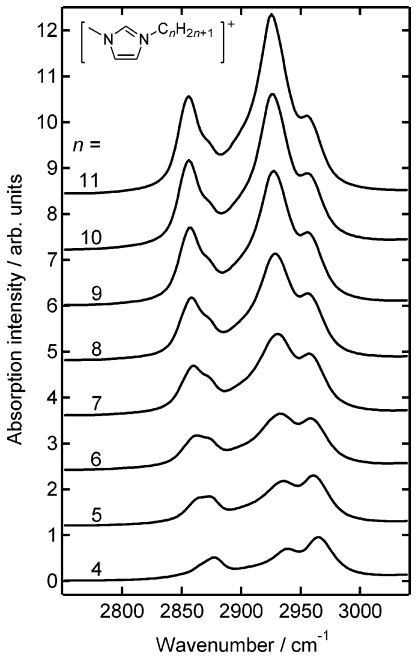

Figure 1. Fourier transform infrared (FTIR) spectra of room-temperature ionic liquids 1-alkyl-3-methylimidazolium tetrafluoroborate ([$C_n$mim]BF_4, $n = 4-11$). For clarity, the base lines of the spectra are shifted by regular intervals. Inset shows the chemical structure of the [$C_n$mim]$^+$ cation.

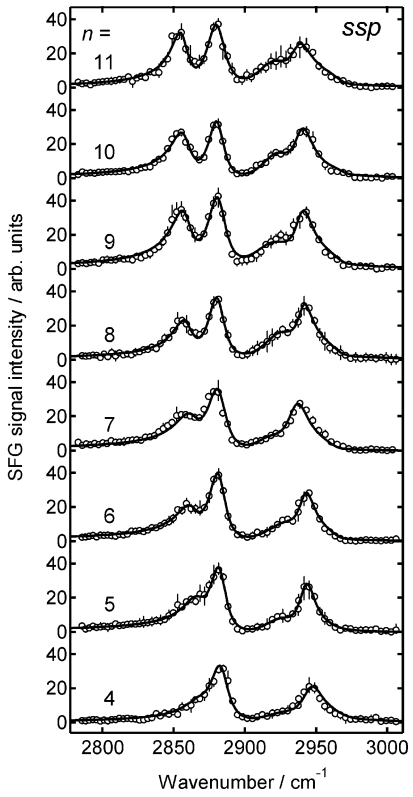

Figure 2. SFG spectra at the air/liquid interface of [$C_n$mim]BF_4 taken at the ssp polarization combination. Open circles with error bars represent data points, whereas solid lines are curve-fitted results.

and averaged using a gated integrator. The wavelength of the IR laser pulse was calibrated using literature values for the rotation−vibration lines of HCl gas at room temperature.[44] HCl shows numerous sharp absorption lines in the range from 2600 to 3000 cm^{-1}. Using a gas cell with an optical path length of 10 cm and a pressure of 2.6×10^4 Pa, we were able to identify 14 vibration−rotation lines in this wavenumber range. All the SFG spectra were normalized to the SFG intensity obtained from a z-cut quartz surface.[45] All the measurements were conducted at 20 °C and in nitrogen gas. The SFG spectra were reproducible during the course of the experiment, which lasted several hours. These results show that the influence of possible contaminates from the nitrogen gas or photodegradation of the liquid sample is insignificant.

The IR spectra of the ionic liquids were recorded using a Fourier-transform IR (FTIR) spectrometer (Mattson, R/S-1). The ionic liquids were held between two KBr windows as a liquid film.

4. Results

4.1. FTIR Spectra of Bulk [$C_n$mim]BF_4 Liquids. Figure 1 shows the FTIR vibrational spectra of [$C_n$mim]BF_4 with $n = 4-11$. The liquid film thickness was inconsistent in the FTIR measurements. Thus, in order to equalize the variations of the optical path length, the spectrum for each [$C_n$mim]BF_4 was normalized to the peak intensity, which maintains a nearly constant absorption coefficient despite the variation in the alkyl chain. We selected the band at 3160 cm^{-1} (not shown in figure), which is assigned to the HCCH symmetric stretching mode of the imidazolium ring.[32]

The bands shown in Figure 1 arise solely from the C−H stretching modes of the alkyl chain in the cation. Band assignments were made on the basis of a previous, but thorough, study on the C−H stretching modes of long *n*-alkyl chains.[46] In the following analysis, the spectrum of [C_{11}mim]BF_4 was selected as a representative of the series of the ionic liquids. The band at 2855 cm^{-1} is assigned to the symmetric C−H stretching mode of the methylene (CH_2) group (designated as d^+); the shoulder band at 2871 cm^{-1} is assigned to the symmetric C−H stretching mode of the terminal methyl group (CH_3) of the alkyl chain (r^+). The band at 2927 cm^{-1} should be the antisymmetric C−H stretching mode of the CH_2 group (d^-). The Fermi resonance of the symmetric stretching mode of CH_3 and the overtone of its bending mode (r^+_{FR}) overlap as a shoulder at ∼2940 cm^{-1}. The band at 2959 cm^{-1} is assigned to the asymmetric C−H stretching mode of the CH_3 group (r^-). There is a faint peak at 2900−2910 cm^{-1}, which may arise from the r^+ mode of the 3-methyl group of the imidazolium ring.

The intensities of both the d^+ and d^- modes monotonically decreased as the length of the alkyl chain decreased. The source of this change can be ascribed to the decreased number of CH_2 groups. On the other hand, the intensities of the r^+, r^+_{FR}, and r^- modes remained nearly constant, which is consistent with the fact that all the ionic liquids have a terminal methyl group in the 1-alkyl chain.

4.2. SFG Spectra of the Air/Liquid Interface of [$C_n$mim]-BF_4. Figures 2−4 show the SFG spectra taken at the ssp, ppp, and sps polarization combinations, respectively. For the all SFG spectra shown here, the intensity was normalized using the reference sample (see Section 3.2). Accordingly, the intensity of the SFG spectra can be compared among the different ionic liquids. The spectra were fitted to eq 1 with the five bands observed in the FTIR spectra. For example, [C_{11}mim]BF_4 shows bands at 2857, 2880, and 2941 cm^{-1}, which can be assigned to the d^+, the r^+, and the r^+_{FR} modes, respectively. The band observed at 2919 cm^{-1} should be due to the d^- mode. In the ssp SFG spectra (Figure 2), the d^+, r^+, d^-, and r^+_{FR} modes of the alkyl chain appear. In the ppp SFG spectra (Figure 3), the band at ∼2975 cm^{-1}, which is assigned to the r^- mode, is

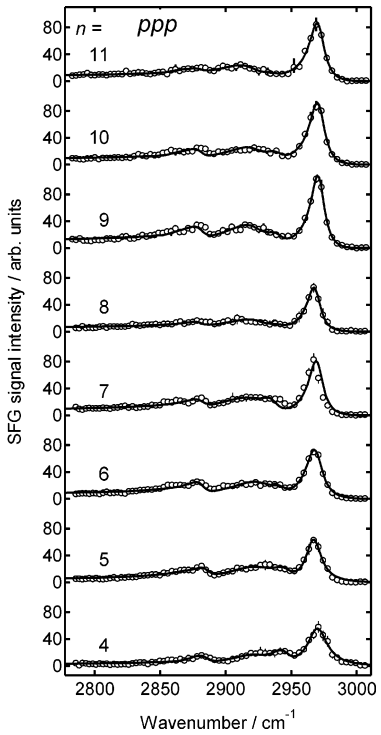

Figure 3. SFG spectra at the air/liquid interface of $[C_n mim]BF_4$ taken at the ppp polarization combination. Open circles with error bars represent data points, whereas solid lines are curve-fitted results.

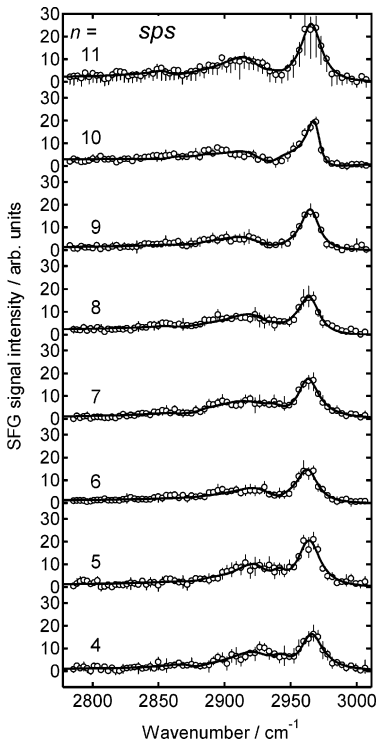

Figure 4. SFG spectra at the air/liquid interface of $[C_n mim]BF_4$ taken at the sps polarization combination. Open circles with error bars represent data points, whereas solid lines are curve-fitted results.

prominent, while the other bands are weaker. In the sps SFG spectra (Figure 4), the peak arising from the r^- mode appears.

4.2.1. CH_2 Symmetric Stretching Mode. The d^+ feature can be a measure of the extent of the disorder in the alkyl chain conformation. For an all-trans alkyl chain, local inversion symmetry due to neighboring methylene groups leads to nearly

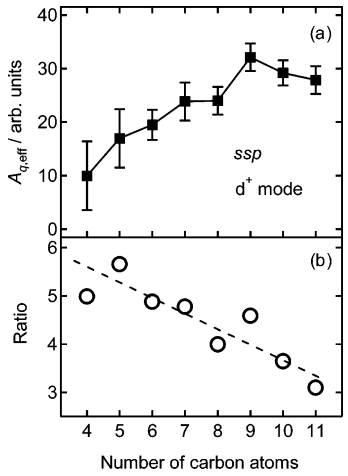

Figure 5. (a) The strength ($A_{q,\mathrm{eff}}$) of the CH_2 symmetric stretching (d^+) mode observed in the SFG spectra taken at the ssp polarization combination versus the number of carbon atoms in the alkyl chain. (b) The ratio of the strength of the d^+ mode to the number of CH_2-CH_2 bonds in the alkyl chain. The broken line is a guide to highlight the dependence on the alkyl chain length.

a zero hyperpolarizability of the d^+ mode.[47] Accordingly, the d^+ feature of the all-trans alkyl chain is weak. However, the strength of the d^+ mode can also depend on the orientational distribution of the CH_2 groups, as shown in eq 3.

Thus, to quantitatively analyze the chain length dependence of the degree of the gauche defect, the orientational distribution of the alkyl chain must be known for each ionic liquid. Actually, it is difficult to simultaneously estimate the orientational distribution and the extent of the gauche defect based on the observed strength of the d^+ mode in the different polarization combinations. However, the SFG spectral features other than the d^+ and d^- modes are similar for all of the ionic liquids. Hence, it is reasonable to approximate that the orientation distribution of the alkyl chain is similar for all of the ionic liquids. Therefore, we can conclude that the strength of the d^+ mode increases as the number of the gauche defects in the alkyl chain increases.

Figure 5a shows the plot of the strength of the d^+ mode observed in the ssp polarization combination versus the alkyl chain length. The strength of the d^+ mode initially increases from $n = 4$ to 9, but then it decreases for $n = 9-11$. If the probability of a gauche defect per CH_2-CH_2 bond is constant for the different alkyl chain lengths, then the percentage of molecules with gauche defects may increase as the alkyl chain length increases. It is unlikely that the observed change in the d^+ mode strength versus the length of the alkyl chain shows such a statistical behavior. The probability of a gauche defect per CH_2-CH_2 bond may be proportional to the d^+ mode strength divided by the number of CH_2-CH_2 bonds in the alkyl chain. Figure 5b shows the ratio of the d^+ mode strength to the number of CH_2-CH_2 bonds as a function of alkyl chain length. The ratio or the probability of a gauche defect appreciably decreases as the length of the alky chain increases. Note that the observed increase of the strength of the d^+ mode and the decrease of the probability of a gauche defect per CH_2-CH_2 bond are consistent with each other. The content of CH_2-CH_2 bonds in the alkyl chain increases with an increase in chain length. Consequently, the increase in the number of the gauche defects may be apparently seen even if the probability of a gauche defect per CH_2-CH_2 bond decreases. The decrease in the probability of gauche defect indicates that the ionic liquids with longer alkyl chains have a propensity to make the conformation of the alkyl chain more ordered.

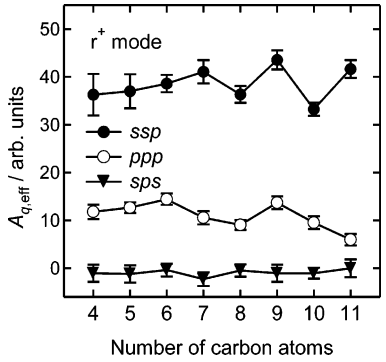

Figure 6. The strength of the CH_3 symmetric stretching (r^+) mode observed in the SFG spectra versus the number of carbon atoms in the alkyl chain.

4.2.2. CH_3 Symmetric Stretching Mode. Figure 6 shows the strengths of the r^+ mode obtained from the SFG spectra shown in Figures 2−4 as a function of the chain length, n. The orientation of the CH_3 group can be calculated by considering the ratio of the strengths of the r^+ mode in two different polarization combinations.[48] Calculating the Fresnel factors in our SFG optical geometry and using eq 2, we finally obtain the ratio between the effective nonlinear susceptibilities as follows:[35]

$$\frac{\chi^{(2)}_{\mathrm{eff,ppp}}}{\chi^{(2)}_{\mathrm{eff,ssp}}} = -0.72 + 1.1 \times \frac{\chi^{(2)}_{ZZZ}}{\chi^{(2)}_{YYZ}} \tag{6}$$

For the r^+ mode of CH_3 group, the ratio between the components of $\chi^{(2)}$ is given by[35,42]

$$\frac{\chi^{(2)}_{ZZZ}}{\chi^{(2)}_{YYZ}} = 2 \times \frac{\gamma\langle\cos\theta\rangle + (1-\gamma)\langle\cos^3\theta\rangle}{(1+\gamma)\langle\cos\theta\rangle - (1-\gamma)\langle\cos^3\theta\rangle} \tag{7}$$

where θ is a tilt angle of the symmetry axis of CH_3 group from the surface normal, and γ is defined by $\gamma = \beta^{(2)}_{\xi\xi\zeta}/\beta^{(2)}_{\zeta\zeta\zeta}$, that is, the ratio between the components of $\beta^{(2)}$ of the CH_3 group. Here, (ξ, η, ζ) is the molecule fixed axis system, where the axis ζ coincides with the symmetry axis, and the axes ξ and η are perpendicular to it. We use $\gamma = 2.5$ obtained from an SFG study of hexadecanol Langmuir monolayer.[42] If the strengths $A_{q,\mathrm{eff}}$ obtained from the fitting of the ssp and ppp spectra are referred to as A_{eff} (ssp) and A_{eff} (ppp), respectively, A_{eff} (ppp)/A_{eff} (ssp) ≈ 0.31 is obtained for $[C_n\mathrm{mim}]BF_4$ with $n = 4-10$. Substituting this value for the left-hand side of eq 6, and assuming a δ-function orientational distribution in eq 7, we have $\theta \approx 52°$. Although $[C_{11}\mathrm{mim}]BF_4$ shows a somewhat exceptional value of the ratio A_{eff} (ppp)/A_{eff} (ssp) ≈ 0.14 and a tilt angle θ of $\approx$45°, every ionic liquid has nearly the same calculated tilt angle for the CH_3 groups. These values are consistent with the reported value for $[C_4\mathrm{mim}]PF_6$ by Baldelli et al.[34]

As is shown in eq 3, the SFG strength of the r^+ mode depends on the orientational distribution of the CH_3 group and N_s. For all the alkyl chains of $n = 4-11$, the strengths of the r^+ mode in the ssp SFG spectra (Figure 6), as well as the calculated tilt angles, do not show significant variation. This observation suggests that the N_s's are also nearly constant for all the ionic liquids investigated. It is pertinent to note that even and odd-numbered alkyl chain lengths for $n = 7-11$ have slightly different r^+ mode strengths. Although the origin of this alternation is currently unclear, it might indicate the presence of a dissimilarity in the orientational distributions of the alkyl chains between the ionic liquids of $n = 4-6$ and $n = 7-11$.

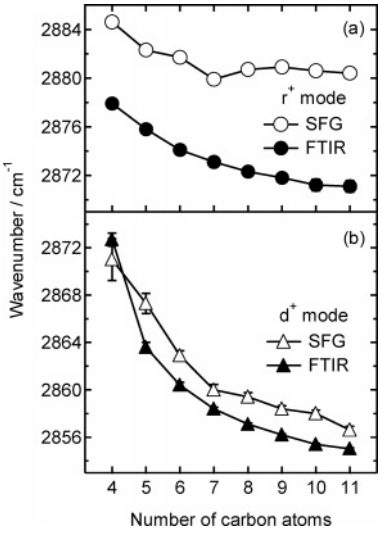

Figure 7. The frequency (in cm^{-1}) of (a) the r^+ mode and (b) the d^+ mode observed in the SFG and FTIR spectra versus the number of carbon atoms in the alkyl chain.

4.3. Frequency of the C−H Stretching Modes in FTIR and SFG Spectra. Figure 7 shows the plot of the frequencies of the r^+ and d^+ modes observed in the SFG and FTIR spectra versus the number of the carbon atoms in the alkyl chain. There are two remarkable features in the frequencies of the r^+ mode (Figure 7a). First, the frequency observed in the SFG spectra is higher than that observed in the FTIR spectra for all the ionic liquids. Second, the frequency of the r^+ mode observed in both the FTIR and the SFG spectra decreases as the chain length increases. The frequency in the FTIR spectra monotonically shifted from 2878 cm^{-1} for $n = 4$ to 2871 cm^{-1} for $n = 11$. The frequency in the SFG spectra also moderately decreased from 2884 cm^{-1} for $n = 4$ to 2880 cm^{-1} for $n = 11$.

Figure 7b shows that the frequency of the d^+ mode also decreased as n increased. A blue shift of the frequency from the bulk liquid to the air/liquid interface can be similarly seen. The difference in the frequencies for each n is smaller than that for the r^+ mode.

5. Discussion

The presence of the r^+ mode frequency shift between the FTIR and SFG spectra allows the microscopic environment of the alkyl chain to be investigated (see Seciton 4.3). One factor that can affect the frequency of a vibrational mode is the dielectric constant of the surroundings. In the energy shift theory, a vibrational mode is modeled as an oscillating dipole, and a higher frequency is predicted if the relevant vibrating group is located in a less polarizable surrounding.[49] Thus, the shift between the frequencies of the r^+ mode observed in the FTIR and the SFG spectra is consistent with the structure in which the terminal CH_3 group of the alkyl chain protrudes from the bulk liquid to the air. This structure agrees with the results of a simulation study on the surface structure of ionic liquids based on the $[C_4\mathrm{mim}]^+$ cation, which demonstrated that the butyl chain tends to face the vacuum side.[50]

Because the differences between the positions obtained from the SFG and the FTIR spectra are not definitively large, we may need to explain the accuracy of the plot shown in Figure 7. The peak positions in the FTIR spectra were obtained by fitting with the Lorentz function. For the SFG data, the resonant

frequencies (ω_2), which were obtained from a least-squares fit, were plotted. As stated in the Experimental Section, we calibrated the wavenumber of the IR laser pulse using the vibration−rotation lines of HCl. Although the observed absorption lines of HCl had fwhm of less than $\approx$7 cm^{-1}, which were probably determined by the energy resolution of the IR pulse, the curves where the SFG and FTIR data are drawn as a function of n are reasonably correlated. Thus, we feel that the shift between the two spectra is a larger magnitude than the experimental error and deserves to be discussed.

In the FTIR spectra, the peak positions of both the r^+ and d^+ modes are red-shifted as n increases (see Figure 7). For the d^+ mode, a similar frequency shift with n has been found in other compounds with long chains: A comprehensive IR vibrational spectroscopy of a solution of a homologous series of *n*-alkanes (represented as (C_mH_{2m+2})) has shown that the frequency of the d^+ mode smoothly decreases from 2862 cm^{-1} for $m = 5$ to 2855 cm^{-1} for $m = 11$.[51] The frequency of the d^+ mode of the ionic liquids varies from 2864 cm^{-1} for $n = 5$ to 2855 cm^{-1} for $n = 11$ (see Figure 7b), which reasonably agrees with that for *n*-alkanes. Therefore, it is likely that the shift of the d^+ mode as the chain length increases is an intrinsic property of alkyl chain. In contrast, the r^+ mode of *n*-alkanes does not show such a frequency change as a function of the number of carbon atoms because the r^+ mode appears at $\sim$2873 cm^{-1}.[51] Other compounds, such as $C_mH_{2m+1}OH$ (i.e., *n*-alcohols) also have nearly constant r^+ mode frequencies.[51] Hence, this red shift in the r^+ mode frequency as n increases may be a characteristic of [$C_n$mim]BF_4. Because the alkyl chain is bonded to the imidazolium cation core, the origin of the shift might be ascribed to the effect of the charge on the cation, and this effect might diminish as the distance between the CH_3 group and the imidazolium ring becomes longer. However, this effect might be excluded because it is unlikely that the terminal CH_3 group in the alkyl chains longer than $n = 4$ is affected by the imidazolium cation core.

The frequency of the r^+ mode observed in the SFG spectra shows a red shift by $\approx$5 cm^{-1} from $n = 4$ to 7 (see Figure 7). This shift can be ascribed to the property of the [$C_n$mim]$^+$ molecules itself, as is seen in the FTIR spectra. On the other hand, the frequency change appears to be very small for the alkyl chains with $n \geq 7$, and the magnitude of the frequency shift from the bulk liquid to the air/liquid interface increases slightly. The dissimilarity of the chain length dependence between the alkyl chains longer and shorter than $n = 7$ is a reminder that a small even−odd alternation exists in the SFG strength of the r^+ mode for [$C_n$mim]BF_4 with $n \geq 7$ (see Figure 6). The even−odd alternation in the SFG strength suggests that a change in the orientational distribution of the alkyl chain appears in an ionic liquid of $n = 7$. Accordingly, the change in the magnitude of the frequency shift might be related to the change in the environment of the CH_3 group due to a change in the orientational distribution of the alkyl chain.

The local structure of bulk crystals and liquids of ionic liquids can provide clues to the surface structure on the basis of intermolecular interactions. To the best of our knowledge, the determination of the single-crystal structure of [$C_n$mim]BF_4 ($n = 4-11$) has not been reported yet. As described in the introduction, the crystal structure analysis of [C_4mim]Cl has shown the presence of a strong chain−chain interaction between the [C_4mim]$^+$ molecules.[20] Raman vibrational spectroscopy of ionic liquids based on the [C_4mim]$^+$ cation by Hamaguchi and co-workers has suggested that a clustering structure similar to the crystal structure exists in the liquid.[20,22] In the ionic liquids based on the [$C_n$mim]$^+$ cation with the alkyl chains of $n \geq 4$, the investigation of the liquid structure using molecular dynamics simulations has shown the formation of a clustering structure of the alkyl chains in the liquid state.[26,27] In particular, it was observed that the nonpolar domains, which originate from the clustering of the alkyl chains, become larger as the alkyl chain length increases.[27] Recent coherent anti-Stokes Raman scattering (CARS) study has also shown that the local structure in [$C_n$mim]BF_4 increases in size as the alkyl chain length increases.[52] In [$C_n$mim]BF_4 with the longer alkyl chains ($n \geq 12$), a thermotropic liquid crystal phase appears at room temperature, and the molecules form lamellar sheet arrays, which separate the ionic group layers from the alkyl chain.[18]

SFG spectroscopy indicates that the alkyl chain of [$C_n$mim]BF_4 has a smaller probability of the gauche defect per CH_2-CH_2 bond as the chain length increases. It has been known that the disorder degree of the alkyl chain at the surface is related to the surface area per molecule. For densely packed surfaces, for example, a thiol self-assembled monlayer on a gold surface and a Langmuir monolayer of long-chain alcohol molecules, it has been shown that the alkyl chain of the molecules has a nearly perfect all-trans conformation.[42,53] However, molecules in loosely packed monolayers, for example, surfactant molecules with a lower surface density and a larger area per molecule, tend to have more disordered chain conformations.[54−56] Thus, it is likely that the interaction between the alkyl chains of neighboring molecules works to straighten the alkyl chain. At the surface of the ionic liquids, if the alkyl chains are far apart from each other, a stronger propensity toward a disordered conformation is expected as the chain length increases than what was observed in this study. This observation suggests that the alkyl chains interact with each other at the air/liquid interface.

It is important to note that there is experimental evidence that both the [$C_n$mim]$^+$ cation and the anion groups share the top surface of the ionic liquid [$C_n$mim]BF_4.[28] A molecular dynamics simulation for [C_4mim]BF_4 has also suggested that the top monolayer at the surface contains both the cation and anion molecules.[50] Because the imidazolium headgroup and BF_4^- anions are rather bulky, a simple structure in which [$C_n$mim]$^+$ cations and BF_4^- anions are homogeneously distributed on the surface would lead to a weak interaction between the alkyl chains. However, the results of the present SFG spectroscopy indicate that the interaction between the alkyl chains plays an important role at the air/liquid interface, which cannot be explained by this simple structure. As a plausible model that consistently explains both the interaction between the alkyl chains and the shearing of the surface by the cation and anion molecules, we propose a structure in which the locally assembled alkyl chains form loose bundles. Although the structure of the bundles is far from rigid, the interaction between the alkyl chains enhances the conformational order in the alkyl chain. The imidazolium cation and BF_4^- anion form an ionic region, and the alkyl chains cluster. In this surface model, the distance between the ionic groups should be insensitive to changes in the alkyl chain length, which is consistent with the observation that there is little change in the N_S of the [$C_n$mim]$^+$ cations upon altering the chain length. In summary, the local structure of the ionic liquids [$C_n$mim]BF_4 can be characterized by the clustering of the alkyl chains both for the bulk liquids and at the interface.

The surface structure of [C_4mim]BF_4 has been investigated using surface probing techniques other than SFG spectroscopy. The result of neutron reflectometry is consistent with a stratified surface structure in which the alkyl chains are separated from the imidazolium cation core and the anion group.[30] An X-ray

reflectivity study has indicated that a 6−7 Å layer exists where the electron density is higher at the surface.[31] It should be noted that, although these measurements are powerful for investigating the density profile across the surface, the structure in the horizontal direction of the surface plane cannot be directly derived. On the other hand, our surface structure model concerns an ordering in the horizontal direction of the surface. This difference may be recalled by comparing these structure models. The result of the neutron reflectometry might partly agree with our conclusion in the sense that the association of the alkyl chains occurs. The X-ray reflectivity measurement has proposed two molecular arrangements. One is a structure in which the butyl chains are arranged parallel to the surface, and the other is with the butyl chains perpendicular to the surface. Although both models represent extreme cases, the latter configuration may possibly be adapted to our surface structural model.

6. Conclusions

We investigated the air/liquid interface of room-temperature ionic liquids $[C_n\text{mim}]BF_4$ with different alkyl chain lengths ($n = 4-11$) using SFG spectroscopy. As the number of carbon atoms in the alkyl chain increases, the probability of a gauche defect per CH_2-CH_2 bond decreases. This result is explained by the enhanced interaction between the alkyl chains with the prolongation of the alkyl chain length. The frequencies of the CH_3 and CH_2 symmetric stretching modes are higher than those in the bulk liquid, which is consistent with an interface structure in which the alkyl chain protrudes from the bulk liquid to the air. As a characteristic local ordering at the air/liquid interface of the ionic liquids, it is proposed that the alkyl chains assemble to form loose bundles.

Acknowledgment. This work was supported in part by Grants-in-Aid for Scientific Research (Nos. 14COEB01, 14GS0213) and by a Grant in Aid for Scientific Research in Priority Area "Science of Ionic Liquids" from the Ministry of Education, Culture, Sports, Science and Technology of Japan. D.K. acknowledges support from KOSEF through Quantum Photonic Science Research Center. Y.O. acknowledges DAIKO Foundation for additional support.

References and Notes

(1) Seddon, K. R. *J. Chem. Technol. Biotechnol.* **1997**, *68*, 351.
(2) Welton, T. *Chem. Rev.* **1999**, *99*, 2071.
(3) Dupont, J.; de Souza, R. F.; Suarez, P. A. Z. *Chem. Rev.* **2002**, *102*, 3667.
(4) Wasserscheid, P.; Keim, W. *Angew. Chem. Int. Ed.* **2000**, *39*, 3772.
(5) Blanchard, L. A.; Hancu, D.; Beckman, E. J.; Brennecke, J. F. *Nature* **1999**, *399*, 28.
(6) van Rantwijk, F.; Lau, R. M.; Sheldon, R. A. *Trends Biotechnol.* **2003**, *21*, 131.
(7) Matsuda, T.; Yamagishi, Y.; Koguchi, S.; Iwai, N.; Kitazume, T. *Tetrahedron Lett.* **2006**, *47*, 4619.
(8) Sekiguchi, K.; Atobe, M.; Fuchigami, T. *J. Electroanal. Chem.* **2003**, *557*, 1.
(9) Matsumoto, H.; Sakaebe, H.; Tatsumi, K. *J. Power Sources* **2005**, *146*, 45.
(10) Garcia, B.; Lavallée, S.; Perron, G.; Michot, C.; Armand, M. *Electrochim. Acta* **2004**, *49*, 4583.
(11) Ue, M.; Takeda, M.; Toriumi, A.; Kominato, A.; Hagiwara, R.; Ito, Y. *J. Electrochem. Soc.* **2003**, *150*, A499.
(12) Kim, Y.; Matsuzawa, Y.; Ozaki, S.; Park, K. C.; Kim, C.; Endo, M.; Yoshida, H.; Masuda, G.; Sato, T.; Dresselhaus, M. S. *J. Electrochem. Soc.* **2005**, *152*, A710.
(13) Hagiwara, R.; Nohira, T.; Matsumoto, K.; Tamba, Y. *Electrochem. Solid-State Lett.* **2005**, *8*, A231.
(14) Noda, A.; Susan, A.; Kudo, K.; Mitsushima, S.; Hayamizu, K.; Watanabe, M. *J. Phys. Chem. B* **2003**, *107*, 4024.
(15) Tokuda, H.; Hayamizu, K.; Ishii, K.; Susan, M. A. B. H.; Watanabe, M. *J. Phys. Chem. B* **2004**, *108*, 16593.
(16) Tokuda, H.; Hayamizu, K.; Ishii, K.; Susan, Md. A. B. H.; Watanabe, M. *J. Phys. Chem. B* **2005**, *109*, 6103.
(17) Gordon, C. M.; Holbrey, J. D.; Kennedy, A. R.; Seddon, K. R. *J. Mater. Chem.* **1998**, *8*, 2627.
(18) Holbrey, J. D.; Seddon, K. R. *J. Chem. Soc. Dalton Trans.* **1999**, 2133.
(19) Fukumoto, K.; Yoshizawa, M.; Ohno, H. *J. Am. Chem. Soc.* **2005**, *127*, 2398.
(20) Saha, S.; Hayashi, S.; Kobayashi, A.; Hamaguchi, H. *Chem. Lett.* **2003**, *32*, 740.
(21) Holbrey, J. D.; Reichert, W. M.; Mieuwenhuyzen, M.; Johnson, S.; Seddon, K. R.; Rogers, R. D. *Chem. Commun.* **2003**, 1636.
(22) Hayashi, S.; Ozawa, R.; Hamaguchi, H. *Chem. Lett.* **2003**, *32*, 498.
(23) Hardacre, C.; Holbrey, J. D.; McMath, S. E. J.; Bowron, D. T.; Soper, A. K. *J. Chem. Phys.* **2003**, *118*, 273.
(24) Katayanagi, H.; Hayashi, S.; Hamaguchi, H.; Nishikawa, K. *Chem. Phys. Lett.* **2004**, *392*, 460.
(25) Hamaguchi, H.; Ogawa, R. *Adv. Chem. Phys.* **2005**, *131*, 85.
(26) Wang, Y.; Voth, G. A. *J. Am. Chem. Soc.* **2005**, *127*, 12192.
(27) Canongia Lopes, J. N. A.; Pádua, A. A. H. *J. Phys. Chem. B 110*, **2006**, 3330.
(28) Law, G.; Watson, P. R.; Carmichael, A. J.; Seddon, K. R. *Phys. Chem. Chem. Phys.* **2001**, *3*, 2879.
(29) Law, G.; Watson, P. R. *Langmuir* **2001**, *17*, 6138.
(30) Bowers, J.; Vergara-Gutierrez, M. C.; Webster, J. R. P. *Langmuir* **2004**, *20*, 309.
(31) Solutskin, E.; Ocko, B. M.; Taman, L.; Kuzmenko, I.; Gog, T.; Deutsch, M. *J. Am. Chem. Soc.* **2005**, *127*, 7796.
(32) Baldelli, S. *J. Chem. Phys. B* **2003**, *107*, 6148.
(33) Fitchett, B. D.; Conboy, J. C. *J. Phys. Chem. B* **2004**, *108*, 20255.
(34) Rivera-Rubero, S.; Baldelli, S. *J. Phys. Chem. B* **2006**, *110*, 4756.
(35) Iimori, T.; Iwahashi, T.; Ishii, H.; Seki, K.; Ouchi, Y.; Ozawa, R.; Hamaguchi, H.; Kim, D. *Chem. Phys. Lett.* **2004**, *389*, 321.
(36) Yoshimura, D.; Yokoyama, T.; Nishi, T.; Ishii, H.; Ozawa, R.; Hamaguchi, H.; Seki, K. *J. Electron Spectrosc. Relat. Phenom.* **2004**, *144−147*, 319.
(37) *Electrochemical Aspects of Ionic Liquids*; Ohno, H., Ed.; Wiley-Interscience: Hoboken, NJ, 2005.
(38) Sheldon, R. *Chem. Commun.* **2001**, 2399.
(39) Chauvin, Y.; Mussmann, L.; Olivier, H. *Angew. Chem. Int. Ed. Engl.* **1995**, *34*, 2698.
(40) Eisenthal, E. B. *Chem. Rev.* **1996**, *96*, 1343.
(41) Richmond, G. L. *Chem. Rev.* **2002**, *102*, 2693.
(42) Zhuang, X.; Miranda, P. B.; Kim, D.; Shen, Y. R. *Phys. Rev. B: Condens. Matter Mater. Phys.* **1999**, *59*, 12632.
(43) Lu, W.; Fadeev, A. G.; Qi, B.; Smela, E.; Mattes, B. R.; Ding, J.; Spinks, G. M.; Mazurkiewicz, J.; Zhou, D.; Wallace, G. G.; MacFarlane, D. R.; Forsyth, S. A.; Forsyth, M. *Nature* **2002**, *297*, 983.
(44) International Union of Pure and Applied Chemistry. Commission on Molecular Structure and Spectroscopy. *Tables of Wavenumbers for the Calibration of Infra-red Spectrometers*; Butterworths: London, 1961.
(45) Wei, X.; Hong, S.; Zhuang, X.; Goto, T.; Shen, Y. R. *Phys. Rev. E: Stat. Phys., Plasmas, Fluids, Relat. Interdiscip. Top.* **2000**, *62*, 5160.
(46) MacPhail, R. A.; Strauss, H. L.; Snyder, R. G.; Elliger, C. A. *J. Phys. Chem.* **1984**, *88*, 334.
(47) Stanners, C. D.; Du, Q.; Chin, R. P.; Cremer, P.; Somorjai, G. A.; Shen, Y. R. *Chem. Phys. Lett.* **1995**, *232*, 407.
(48) Sung, J.; Jeon, Y.; Kim, D.; Iwahashi, T.; Iimori, T.; Seki, K.; Ouchi, Y. *Chem. Phys. Lett.* **2005**, *406*, 495.
(49) Herzberg, G. *Molecular Spectra and Molecular Structure II. Infrared and Raman Spectra of Polyatomic Molecules*; Van Nostrand: New York, 1945, p. 534.
(50) Lynden-Bell, R. M.; Del Pópolo, M. *Phys. Chem. Chem. Phys.* **2006**, *8*, 949.
(51) Nyquist, R. A. *Interpreting infrared, raman, and nuclear magnetic resonance spectra*; Academic Press: San Diego, 2001; Vol 1.
(52) Shigeto, S.; Hamaguchi, H. *Chem. Phys. Lett.* **2006**, *427*, 329.
(53) Nishi, N.; Hobara, D.; Yamamoto, M.; Kakiuchi, T. *J. Chem. Phys.* **2003**, *118*, 1904.
(54) Bell, G. R.; Bain, C. D.; Ward, R. N. *J. Chem. Soc. Faraday Trans.* **1996**, *92*, 515.
(55) Guyot-Sionnest, P.; Hunt, J. H.; Shen, Y. R. *Phys. Rev. Lett.* **1987**, *59*, 1597.
(56) Miranda, P. B.; Pflumio, V.; Saijo, H.; Shen. Y. R. *Thin Solid Films* **1998**, *327−329*, 161. Walker, R. A.; Conboy, J. C.; Richmond, G. L. *Langmuir* **1997**, *13*, 3070. Yang, C. S.-C.; Richter, L. J.; Stephenson, J. C.; Briggman, K. A. *Langmuir* **2002**, *18*, 7549.